International Research Journal of Advanced Engineering and Science
ISSN (Online): 2455-9024

Assessing Flow Bends in Open Channels

Shaimaa S. Abdou[1], Ashraf M. ElMoustafa[1], Mahmoud Samy[1]
[1]Irrigation and Hydraulics Department, Faculty of Engineering, Ain Shams University, Cairo, Egypt

Abstract**—** *The cost and time of physical experiments motivated the researchers to explore the capability of numerical models. Accordingly, this research was commenced with the assessing flow in open channel bends. A numerical model FLUENT was implemented to scrutinize flow features in the sharply open channel bend 193°, where large-eddy-simulation "LES" used as a turbulent model. The formed eddies were directly solved, while the smaller scale eddies were statistically modeled. The model was validated against experimental results of one of previous study K. Blanckaert (Q89), where his experiments investigated the interaction between stream flow and secondary flow. The research designated that the computed super-elevation, stream velocity and transversal velocity were in good accordance to experimental results of K. Blanckaert (Q89). In addition, LES predict "outer-bank cell". The research confirmed that the secondary flow cell originates at the outer bank and rotates opposite to the main secondary cell, which is considered the main cause for bank erosion process as shown in research reviews.*

Keywords**—** *Large- eddy-simulation; Numerical model; Open-channel-sharp-curve; Secondary-flow; Turbulent model*.

I. INTRODUCTION

Secondary flows occur in curved open channel reaches, where centrifugal forces and pressure gradient are in imbalance. The interactions between these two forces leading to Increment of energy loss, development of outer bank erosion, formation of bed-point-bar at inner bank, creating of meandering, establishment of low-separation-zones, development of flow-recirculation-zone, and reduction in channel capacity (Shiono et al. 1999; Roca et al. 2007; Blanckaert 2015).

Regarding the scrutinized literature, it was clear that the flow characteristics along the curved open channel for many investigations are difficult to achieve experimentally, especially at boundaries (i.e. sidewalls) in addition to the spatial resolution and accuracy of measuring are low (Blanckaert and Graf 2004;Tang and Knight 2015). Therefore, one of the main benefits of the numerical simulation for curved open channel is the transferring of intermit-tent laboratory measurements to the integrated velocity field and reaching to the difficult areas.

Although, the modern computer allows solving complex equations, nevertheless, there are still lacks in studying of the hydrodynamic processes occurring near the banks, the flow characteristics as the velocity distribution, and secondary flow inside the curved channels reaches by using the different turbulent model.

The objective of this research is simulating of the key features of flow as super-elevation and velocity distribution using FLUENT software and applying the LES turbulent model, and checking the capability of this model to simulate this type of flow and this sharply open channel bend by validating the predicted results from the numerical model with the results of K. Blanckaert's experiment (Q89).

Regarding the assembled literature, it was clear that several experimental studies have been conducted on curved open channel to examine flow characteristics, especially; two important subjects that were repetitively addressed: the strength of the secondary cells (Wei et al. 2016, Vaghefi et al. 2016) and the interactions between the secondary flow pattern and the main flow (De Vriend, 1981, Tang and Knight 2015).

Studies, particularly focus on curved open-channel flow, have been first published by pioneer as Rozovskii (1957) in which he conducted on trapezoidal open channels and noticed that the secondary flow generated in the bend with angles at least 100 degree in shallow channel and 180 degree for the deep ones..

In the recent era, Blanckaert and de Vriend (2003 & 2004 & 2005) conducted series of experiments on curved open-channel flows in order to investigate the flow characteristics in the channel bend and the cross-stream velocity and observed maximum velocities occur near the circulation cells below the surface, in the same context, Pradhan et al. (2018) investigated experimentally the flow characteristics in 193° sharp bend under variable parameters (i.e. water depth, bed, discharges, wall friction) and they deduced that the effect of bend is more on a smoother channel above a certain depth and the transition sections..

Sui et al.(2006) assessed local the impact of Froude Number on the shaping of the secondary flow and its strength and scour in open channels in a 90o bend in addition to Roca et al. (2009) noticed that the maxi-mum velocities increases from the bend entry until the cross-sections from 40° to 60° inside the curve.

Accordingly, numerical simulation is an important avenue to go through because of it is more advantageous than experimental work, in terms of cost and time, it could assess the integrated velocity field in problematic areas, it could solve complex equations.

A few numerical models were implemented to calculate the flow characteristics of sharp open channel bends and fewer using FLUENT software. Gholami et al. (2014) applied the CFD with K-ε turbulent model and the results showed that models are reasonably accurate to simulate flow characteristics. Zeng et al.(2010); Huang et al.(2009); and Zeng et al. (2008) used RANS Code to predict the flow characteristics in the curved open channel. Bodnar and Prihoda (2006) used k-ω turbulence model to analyze the free surface slope in the sharp bend, and Stoesser et al. (2008) have applied LES on a meandering open channel flow and pointed on the flow manner near the bed.

II. MATERIALS AND METHODS

In order to achieve the research objectives, a methodology was designed as shown below.

Shaimaa S. Abdou, Ashraf M. ElMoustafa, and Mahmoud Samy, "Assessing Flow Bends in Open Channels," *International Research Journal of Advanced Engineering and Science*, Volume 6, Issue 2, pp. 49-54, 2021.

International Research Journal of Advanced Engineering and Science
ISSN (Online): 2455-9024

Previous Experimental Investigation by Blanckaert

During his investigation, experimental set up and experimental measurements, were expounded. The geometry of the experimental setup is shown in Figure 1 and carried out by Blanckaert 2002a at Ecole Polytechnique Fédérale de Lausanne EPFL of flume. Concerning the experimental set up, an experimental 22.7 m long smooth vertical PVC flume, with a bed slope of 0.22% was constructed; Fig. 1.

The experimental hydraulic conditions are listed in Table 1.

Focusing on the experimental measurements, they are listed, as follows:

- Measurements were observed to the water levels, bed levels and flow velocities in the cross-sections at angles of 15, 30, 60, 90, 120, 150 and 180o; Figure 1b.
- Measurements were recorded US (upstream) the bend in the straight reach, at 2.5 and 0.5 m, while they were observed DS (downstream) the bend in the straight reach, at 0.5, 1.5, 2.5 and 3.5 m.
- Measurements were carried in the bend at n = from -0.5, -0.475, -0.45, - 0.425, -0.4, -0.375, -0.35, -0.325, -0.3, -0.25, -0.2, -0.15, -0.1, -0.05, 0, 0.05, 0.1, 0.15,0.2, 0.25, 0.3, 0.325, 0.35, 0.375, 0.4, 0.425, 0.45, 0.475, 0.5 m.

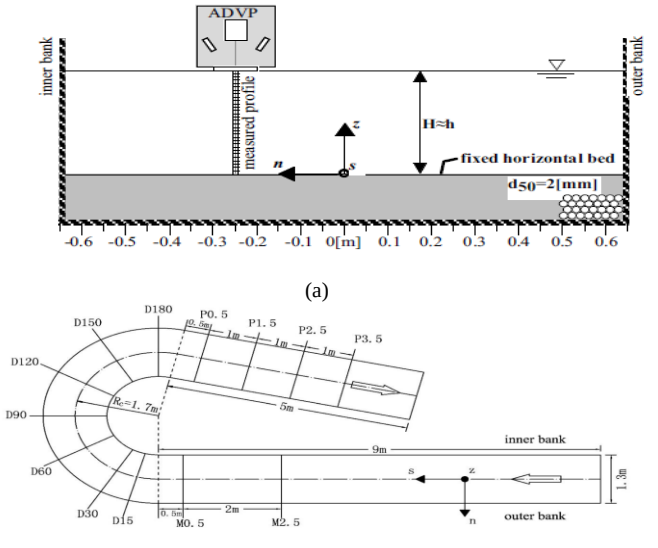

Fig. 1. Experimental flume (a) elevation and (b) plan with the measured locations

A curvilinear reference system (i.e. s, n and z) is adopted, where (s) designates stream direction, (n) denotes transverse outward direction and (z) signposts upward direction.

TABLE I. Experimental hydraulic condition

Q (l/s)	H (m)	U (m/s)	u* (m/s)	Cf (-)	Re (103)	Fr (/)	R/B (/)	H/R (/)	B/H (/)
89	0.159	0.43	0.040	0.0086	69	0.35	1.31	0.094	8.2

Where:

B= Width of flume (m),
H= Average flume depth (m),
R= Radius of curvature (m),
U= Flume average velocity (m/s),
u*= Flume average shear velocity (m/s),
Q= Discharge (l/s),
Cf= Chezy friction factor,
Re= Reynolds number, and
Fr= Froude number

Numerical Investigation

In the present numerical investigation, FLUENT software was implemented, where it is implemented and accepted worldwide. The calculation proceeds at discrete locations described by a numerical grid. The solution accuracy depends on the discretization method. The equations are solved by algorithms until convergence is attained, as elaborated in FLUENT manual.

This section elaborates FLUENT conceptual phases, the basic equations, the internal computation and boundary conditions, as follows:

Regarding the *Conceptual phases* of LES, they employ spectral filtering to separate larger from smaller eddies. This is achieved as follows:

1. A filter is designated to decompose velocity field into the sum of a resolved component and sub-grid (SGS),
2. Establish Navier stokes filtered equations that are similar to original equations, except for a residual sub-grid stress term, arising from filtering, and
3. Mimic the sub-grid by a sub-grid model.

Focusing on the *basic equations* of LES, they are described by Navier Stokes equations with a cylindrical-coordinate-system (r, θ and z) and velocity components (u, v and w). The equations are presented in equations (1) to (5), as follows:

Continuity

$$\frac{1}{r}\frac{\partial(ru)}{\partial r}+\frac{1}{r}\frac{\partial v}{\partial \theta}+\frac{\partial w}{\partial z}=0 \quad (1)$$

Momentum in r-direction

$$\frac{\partial u}{\partial t}+\frac{1}{r}\frac{\partial(ruu)}{\partial r}+\frac{1}{r}\frac{\partial(vu)}{\partial \theta}+\frac{\partial(wu)}{\partial z}-\frac{v^2}{r}=-\frac{\partial P}{\partial r}+\nu\left(\nabla^2 u-\frac{u}{r^2}-\frac{2}{r^2}\frac{\partial v}{\partial \theta}\right) \quad (2)$$

Momentum in θ-direction

$$\frac{\partial v}{\partial t}+\frac{1}{r}\frac{\partial(ruv)}{\partial r}+\frac{1}{r}\frac{\partial(vv)}{\partial \theta}+\frac{\partial(wv)}{\partial z}+\frac{uv}{r}=-\frac{1}{r}\frac{\partial P}{\partial \theta}+\nu\left(\nabla^2 v-\frac{v}{r^2}+\frac{2}{r^2}\frac{\partial u}{\partial \theta}\right) \quad (3)$$

Momentum in Z-direction

$$\frac{\partial(w)}{\partial t}+\frac{1}{r}\frac{\partial(ruw)}{\partial r}+\frac{1}{r}\frac{\partial(vw)}{\partial \theta}+\frac{\partial(ww)}{\partial z}=-\frac{\partial P}{\partial Z}+\nu\nabla^2 w \quad (4)$$

$$\nabla^2=\frac{1}{r}\frac{\partial}{\partial r}(r\frac{\partial}{\partial r})+\frac{1}{r^2}\frac{\partial^2}{\partial \theta^2}+\frac{\partial^2}{\partial z^2} \quad (5)$$

Where:

u=velocity component, in Cartesian-system, in x-direction
v=velocity component, in Cartesian-system, in y-direction
w=velocity component, in Cartesian-system, in y-direction
t=time
P=pressure
a=acceleration due to gravity
ρ=density

Concentrating on the ***internal computation***, the sub-grid modeling calculates large-scale behavior by parameterizing the small-scale performance. WALE Wall model was adapted

Shaimaa S. Abdou, Ashraf M. ElMoustafa, and Mahmoud Samy, "Assessing Flow Bends in Open Channels," *International Research Journal of Advanced Engineering and Science*, Volume 6, Issue 2, pp. 49-54, 2021.

International Research Journal of Advanced Engineering and Science
ISSN (Online): 2455-9024

and implemented to mimic the eddy viscosity, where it was created to rectify wall-asymptotic-performance.

Converging on the boundary conditions, four boundaries were implemented for the bend (i.e. inlet, outlet, walls and surface); Fig. 2 (a). The mass flow inlet boundary was adopted as the water inlet; sidewalls so as bed are mimicked as no-slip-wall boundary condition. A pressure outlet boundary-condition is implemented to allow free-air flow, and the top of the channel (water surface utilized a pressure outlet-boundary-condition.

TABLE II. Boundary conditions

Boundary Conditions	Type of Boundary Conditions	Values
Inlet	Mass flow inlet	89 kg/s
Outlet	Pressure outlet	Atmospheric pressure
Free surface	Pressure outlet	Atmospheric pressure
Bed and walls	Wall	

In earlier Blanckaert's experiments, it was noticed that the flow characteristics change inside the bend. These changes gradually fade into the straight reaches for a distance upstream and downstream of the bend of about 1.5 m, whereas the radius of bend and the influence of centrifugal forces vanished in the straight reaches, and thus, the computational domain (the simulated volume) is reduced as shown in Fig. 2b to minimize the number of nodes and the mesh size and hence the simulation time.

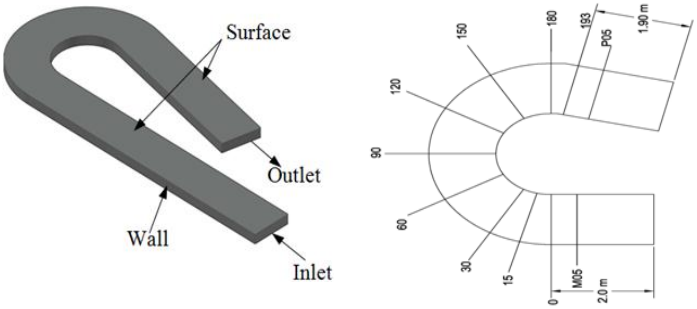

(a) (b)

Fig. 2. (a) Boundary Conditions and (b) Computational Domain

III. Results and Discussion

In CFD, there are several ways to handle the free-surface boundary. The easiest approach is to "ignore" free surface deformations and performing of the rigid lid approximation because of computing free-surface deformations for instance at every distance and time step is more complicated as was stated by Constantinescu et al. (2011); Paik and Sotiropoulos (2005), they showed that the rigid lid approximation is only applicable to low Froude number (i.e. $Fr \leq 0.5$) flows.

In this study, the free surface is treated by the rigid lid model due to the low Froude number as shown in table 1, as known that the water inside open channel is discharged under gravity. Thus, the water levels have been computed as Equation (6):

$$\frac{\partial h}{\partial r} = \frac{1}{\rho g}\left(\frac{\partial p}{\partial r}\right) \qquad (6)$$

Throughout this investigation, results were analyzed and discussed, in terms of water depth and secondary circulation cells velocity. Concentrating on the water depth, the water levels were computed using equation (6), while Figure 3 presents the experimental and numerical results, respectively. On the other hand, Figure 4 presents the measured versus the computed levels for the different cross sections, while Figure 5 presents the measured and computed water depth changes along the channel.

Figures 3, 4,& 5 showed that the water surface slope, in the transverse direction (n), is generated to reduce the centrifugal force. This imbalance between the centrifugal force and the pressure gradient created a secondary circulation in the bend.

In the different sections, slight water depth changes occurred before the bend, by a distance of 0.5 m and after the bend, by a distance of 0.5 m. This is attributed to the fact of the curvature discontinuity. On the other hand, tangible water depth changes occurred within the bend, where the surface raises at the outer bank and falls at the inner bank. This generated secondary flow that vanishes outside the bend. Figures 3 &4 designated the good agreement between the numerical and experimental results of Blanckaert.

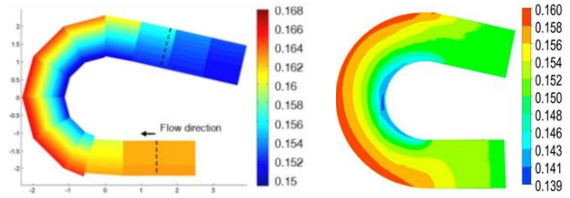

(a) (b)

Fig. 3. Water depths all over the channel (a) measured and (b) computed

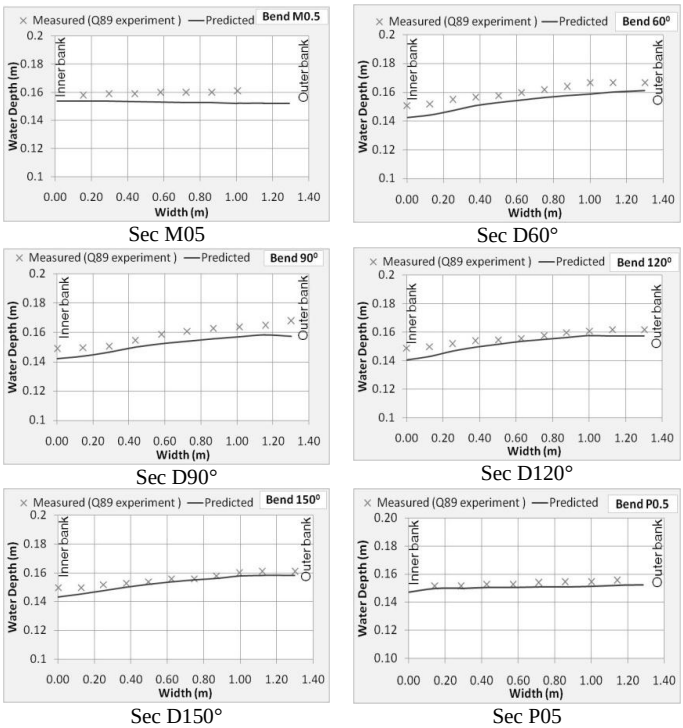

Sec M05 Sec D60°

Sec D90° Sec D120°

Sec D150° Sec P05

Fig. 4. Measured versus computed water depths at different sections

Shaimaa S. Abdou, Ashraf M. ElMoustafa, and Mahmoud Samy, "Assessing Flow Bends in Open Channels," *International Research Journal of Advanced Engineering and Science*, Volume 6, Issue 2, pp. 49-54, 2021.

International Research Journal of Advanced Engineering and Science
ISSN (Online): 2455-9024

Fig. 5 designated that the measured and computed water levels, *along the channel*, were in good agreement with slight underestimation, since the root mean square error (RMSE) between the measurements and predicted results ranges from 0.09 (at section M05) to 0.24 (at section D150).

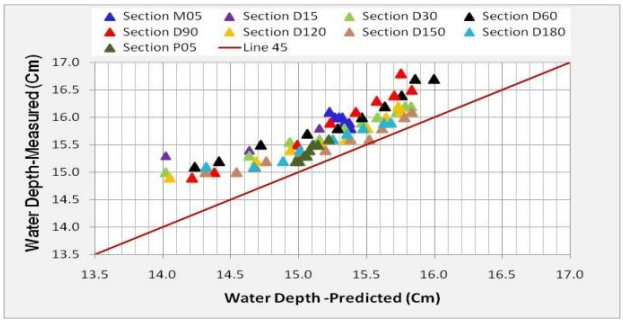

Fig. 5. Measured versus computed water depths along the channel

By comparing between the water depths measurement and predicting along the channel as shown Figure 5, the results revealed that the maximum difference between the outer and the inner banks in water depths occurs around sections D60˚ and D90˚in both experiment and model as shown above with red and black colors.

From Figures 4& 5, it is concluded that the slope of water surface is non linear in all sections in which the slope in the inner half of the bend is greater than its outer half. This conclusion is matching with conclusions of Bodnar and Prihoda (2006), in which they studied the channel bend numerically by using k -ε turbulent model and is inconsistent with conclusion of De Vriend and Geldof (1983), in which they studied the bend numerically and stated that the slope of water level is linear.

Focusing on the *velocity distribution*, it is distinguished in curved open channel by a maximum velocity that shifts /migrates from a bank to another. The velocity distributions were computed and Figure 6 presents the measured depth averaged velocity of the experimental so as numerical results, respectively. On the other hand, Figure 7 presents the measured versus the computed velocities for the different profiles, while Figure 8 presents the measured and computed stream velocity all over the channel, for D90º at z/h=1 at the water surface and z/h=0 on the bed. Figure 9 presents the measured and computed stream velocity all over the channel, for D90o, at z/h=1(at the water surface) and z/h=0 (on the bed).

Regarding the *stream velocity*, .Fig. 6 showed that once the flow enters the bend, the velocity increases towards the inner bank, a separation zone is generated, and a potential vortex is formed, On the other hand, once the flow exits the bend, a forced vortex is generated. This is attributed to the fact that rapid curvature change plays a significant role in outward velocity distribution as stated in many researches. Moreover, the predicted results by FLUENT is over-estimated the velocities by 14% higher than measurement values.

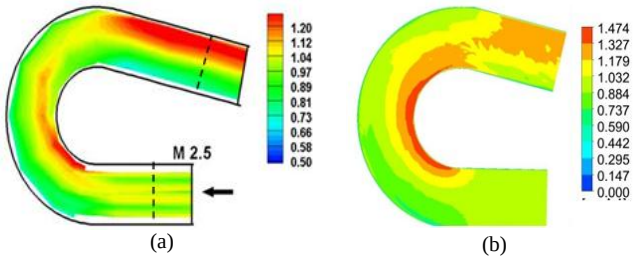

Fig. 6. Contour map for stream velocity all over the channel (a) measured (b) Computed

Fig. 7, From n=-0.5 up to n=0 (half of the bend from inner bank to center) in all section, the stream velocity at the upper part is reduced and at the bottom part is increased then flow separation is generated, while from n=0 up to n=+0.5 (half of the bend from center to outer bank), the reduction shifted to the center and then gradually shifted slightly to the outer bank. The measured and computed stream velocities results were in good agreement as shown in Fig.7, all over the different sections. The figures also indicated that once the flow into the bend, the velocity reduction migrates towards the center and shifts to the outer bank.

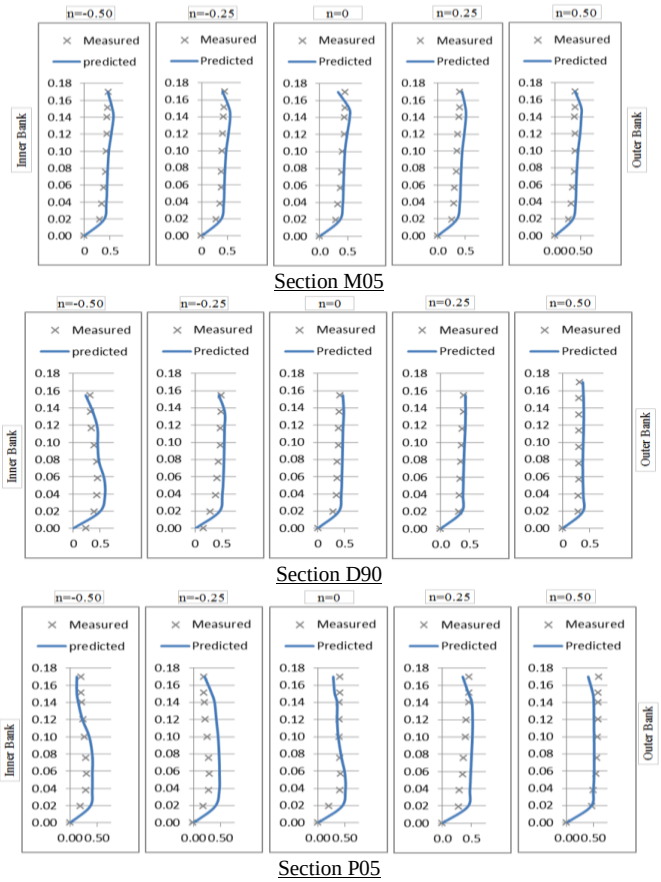

Fig.7. Measured versus computed stream velocity profiles for the different sections

For more clarity and understanding the flow behavior in the bend, Figure 8 flagged out that the measured and computed velocity distributions, for D90º at z/h=1 at the Water surface and z/h=0 on the bed, are in good agreement

Shaimaa S. Abdou, Ashraf M. ElMoustafa, and Mahmoud Samy, "Assessing Flow Bends in Open Channels," *International Research Journal of Advanced Engineering and Science*, Volume 6, Issue 2, pp. 49-54, 2021.

International Research Journal of Advanced Engineering and Science
ISSN (Online): 2455-9024

and showed that the maximum stream velocities occurred at the inner bank at left due to change in pressure gradient.

Fig. 9 presents the measured and computed stream velocity all over the channel, for P05, at z/h=1(at the water surface) and z/h=0 (on the bed). Apparent was that the maximum velocities occur at the outer bank at the right and that highest velocity shifted from the inner bank to outer bank due to outer secondary flow cells at the bend exit.

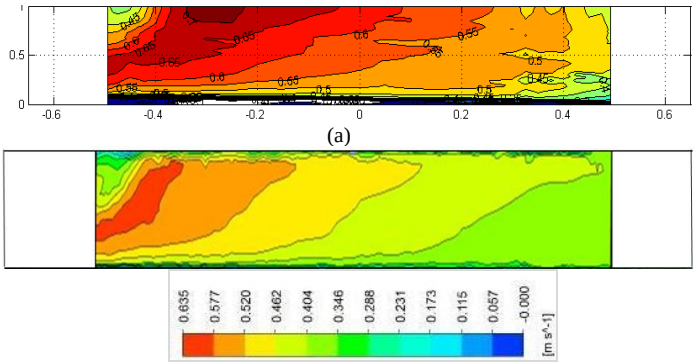

(a)

(b)

Fig. 8. a) Measured versus b) computed stream velocity distributions at water surface (forD90º at z/h=1 at the Water Surface and z/h=0 on the bed)

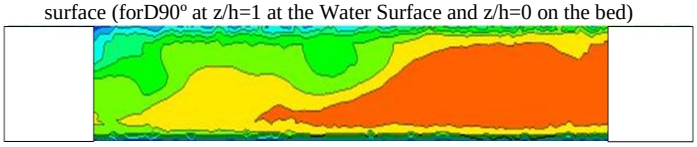

Fig. 9. Computed stream velocity at the water surface (for P05 at z/h=1 at the water surface and z/h=0 on the bed)

Regarding the *transversal velocity*, Fig.10, From n=-0.5 up to n=0 (half of the bend from inner bank to center) in all section, the transverse velocity increased and reached to its maximum value in the section D90° and sequentially while from n=0 up to n=0.5 (half of the bend from center to outer bank), decreased up to half its value at section P05.

Fig.10 indicated that the computed transverse velocities were underestimated for the bend entrance and more researches are needed to spot the reasons for this underestimated value by model (FLUENT) at the bend entrance. On the other hand, the computed results were similar to the measured values after the bend. LES model succeeded in capturing the main features of the secondary cross-stream circulation cells. These cells are characterized by outward transverse velocities in the upper and inward transverse velocities in lower part of the water column in sections D90° and P05

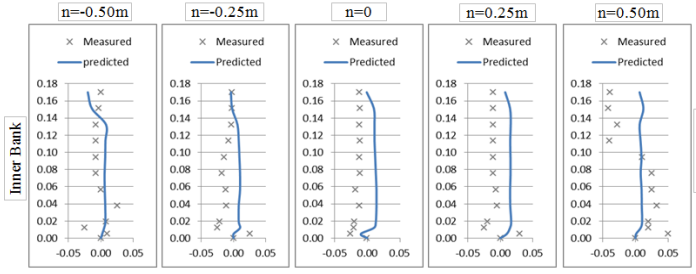

Section M05

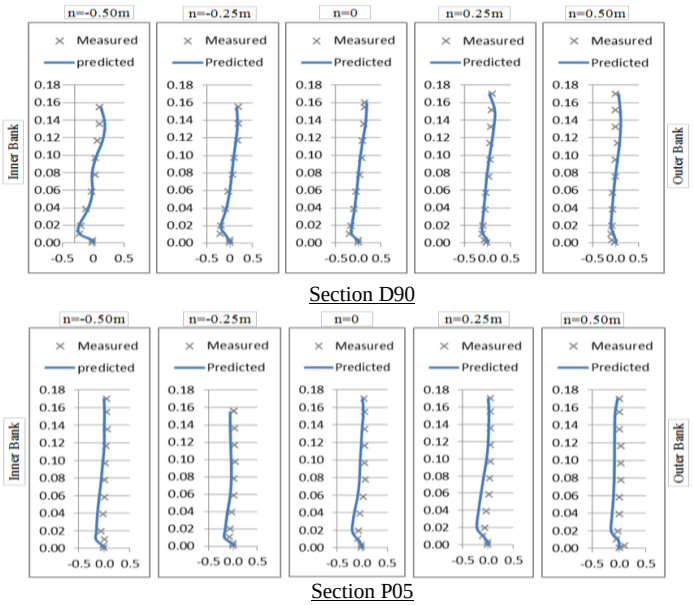

Section D90

Section P05

Fig. 10. Measured and computed transversal velocity at different sections

For more clarity and understanding the flow behavior in the bend, Fig. 11 presents the measured and computed transverse velocities for D90º at z/h=1(at the water surface) and z/h=0 (on the bed), where the main secondary circulation cell is fully developed and its intensity increases close to the inner bank. Also, obvious was that FLUENT provided results similar to the measured values for D90°. FLUENT overestimated the values by 17% compared to measurements.

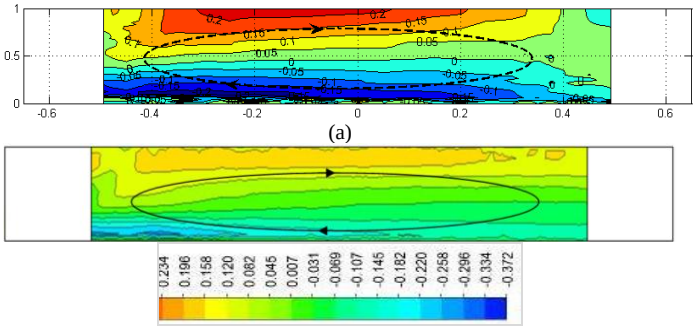

(a)

(b)

Fig. 11. a) Measured and b) computed transverse velocity at different sections (for D90º at z/h=1 at the water surface and z/h=0 on the bed)

Regarding the *secondary circulation*, in the curved open channel, two circulation cells are generated. Main secondary circulation cell (centre-region cell of secondary flow) which are fully developed at section D90° and the other is outer circulation cell which produced by the water surface and the outer bank at the upper half of outer bank at P05 section (after 0.5 m from the bend exit) beside the main secondary circulation cell. Fig. 12 presents two secondary circulation cells. The outer bank cell rotates opposite to the center circulation cell of secondary flow. The velocities at the water surface are diverted away from the outer bank.

Regarding the secondary flow, the predicted results by FLUENT is matched with Vaghefi et al. (2016) research where he stated that the occurrence of maximum secondary

Shaimaa S. Abdou, Ashraf M. ElMoustafa, and Mahmoud Samy, "Assessing Flow Bends in Open Channels," *International Research Journal of Advanced Engineering and Science*, Volume 6, Issue 2, pp. 49-54, 2021.

flow strength at the second half of the bend and the main cause for the erosion of the bank is the outer bank cell.

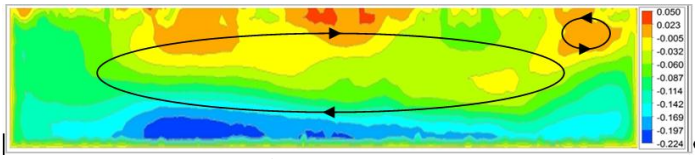

Fig. 12. Contour Map for Two circulation cells at section P05

IV. CONCLUSIONS

In this paper, FLUENT software with LES turbulent model have been used to study the flow features inside a strongly-curved 193° open channel bend.

It can be concluded that FLUENT software with LES model is capable of predicting results for the produced super-elevation, stream and transverse velocities, predicting the two secondary circulation cells (main and outer bank cells) in the sharply open channel bend, and a good visualization for these cells and hence, it is recommended for further investigation for transverse velocities because the prediction by model was slightly underestimate at some sections and the proposed solutions to solve problems associated with flow through channel bends.

REFERENCES

[1] Blanckaert K and de Vriend H J. "Non-linear modeling of mean flow redistribution in curved open channels." Water Resources Research, vol. 39, 2003.
[2] Blanckaert K and de Vriend H J. "Secondary flow in sharp open-channel bends." Journal of Fluid Mechanics, vol. 498, 353–380, 2004.
[3] Blanckaert K and de Vriend H J. "Turbulence structure in sharp open-channel bends." Journal of Fluid Mechanics, vol. 536, 27-48, 2005.
[4] Blanckaert, K.. "Flow separation at convex banks in open channels." Journal of Fluid Mechanics, vol. 779, 432–467, 2015.
[5] Blanckaert, K.; Graf, W.H., "Momentum Transport in Sharp Open-Channel Bends." Journal of Hydraulic Engineering, vol.130, 186–198, 2004.
[6] Blanckaert, K. "Secondary currents measured in sharp open-channel bends" River Flow 2002, Louvain, Belgium, 2002a.
[7] Bodnar T, Prihoda J. "Numerical simulation of turbulent free-surface flow in curved channel" Flow Turbulence Combust vol. 76, 429-442, 2006.
[8] Constantinescu G, Koken M, and Zeng J. "The structure of turbulent flow in an open channel bend of strong curvature with deformed bed: Insight provided by detached eddy simulation" Water Resources Research vol.47, 1-17, 2011.
[9] De Vriend, H.J. "Velocity redistribution in curved rectangular chanels." Journal of Fluid Mechanics, vol. 107, 423-439, 1981.
[10] De Vriend, H.J.; Geldof, H.J. "Main flow velocity in short and sharply curved river bends" Delft University of Technology, vol.17, 1-14,1983.
[11] Gholami A, Akhtari A A, Minatour Y, Bonakdari H, Javadi A A. "Experimental and numerical study on velocity fields and water surface profile in a strongly-curved 90 open channel bend." Journal of Engineering Applications of Computational Fluid Mechanics, vol. 8, 447-461, 2014.
[12] Huang SL, Jia YF, Chan HC, Wang SSY "Three-dimensional numerical modeling of secondary flows in a wide curved channel" Journal of Hydrodynamics, vol. 21, 758-766, 2009.
[13] Paik J and Sotiropoulos F. "Coherent structure dynamics upstream of a long rectangular block at the side of a large aspect ratio channel" Physics of Fluids, vol.17, 1-14, 2005.
[14] Pradhan A, Khatua K K, and Sankalp S. "Variation of velocity distribution in rough meandering channels" Advances in Civil Engineering, vol.40, 2018.
[15] Roca, M.; Martín-Vide, J.P.; Blanckaert, K. . "Reduction of Bend Scour by an Outer Bank Footing: Footing Design and Bed Topography." Journal of Hydraulic Engineering, vol. 133, 139–147, 2007.
[16] Rozovskii, I.L. "Flow of Water in Bends of Open Channels", 2nd ed.; Academy of Sciences of the Ukrainian SSR, 1957.
[17] Roca, M.; Blanckaert, K.; Martín-Vide, J.P. "Reduction of Bend Scour by an Outer Bank Footing: Flow Field and Turbulence". Journal of Hydraulic Engineering, vol. 135, 361–368, 2009.
[18] Shiono, K.; Muto, Y.; Knight, D.W.; Hyde, A.F.L.. "Energy losses due to secondary flow and turbulence in meandering channels with overbank flows." Journal of Hydraulic Research, vol. 37, 641–664, 1999.
[19] Sui J, Fang D, and Karney B W "An experimental study into local scour in a channel caused by a 90° bend" Canadian Journal of Civil Engineering, vol.33, 902-911, 2006.
[20] Stoesser, T., Ruether, N. & Olsen, N. R. B. "Near-bed flow behaviour in a meandering channel" River Flow 2008: 4th International Conference on Fluvial Hydraulics , 793–799, 2008.
[21] Tang, X.; Knight, D.W. "The lateral distribution of depth-averaged velocity in a channel flow bend."Journal of Hydro-environment Research, vol.9, 532–541, 2015.
[22] Vaghefi, M.; Akbari, M.; Fiouz, A.R. "An experimental study of mean and turbulent flow in a 180 degree sharp open channel bend: Secondary flow and bed shear stress. "KSCE Journal of Civil Engineering, vol. 20, 1582–1593, 2016.
[23] Wei, M.; Blanckaert, K.; Heyman, J.; Li, D.; Schleiss, A.J. "A parametrical study on secondary flow in sharp open-channel bends: Experiments and theoretical modelling. "Journal of hydro-environment research, vol.13, 1–13, 2016.
[24] Zeng J, Constantinescu G, Weber L "3D calculations of equilibrium conditions in loose-bed open channels with significant suspended sediment load" ASCE Journal of Hydraulic Engineering, vol. 136, 557–571, 2010.
[25] Zeng J, Constantinescu G, Weber L. "A 3D nonhydrostatic model to predict flow and sediment transport in loose-bed channel bends" Journal of Hydraulic Research, vol.46, 356-372, 2008